Convolutional Neural Networks-Based Sea Ice Detection From TDS-1 Data

Qingyun Yan, *Student Member, IEEE*, and Weimin Huang, *Senior Member, IEEE*
Faculty of Engineering and Applied Science, Memorial University
St. John's, Newfoundland, Canada
Email: qy2543@mun.ca, weimin@mun.ca

***Abstract*—This paper presents a convolutional neural networks (CNNs)-based scheme for sea ice detection from TechDemoSat-1 (TDS-1) delay-Doppler maps (DDMs). DDM images were employed as input and SIC data from passive microwave sensors were modified as targeted output. Two different CNNs were designed and tested with the full-size DDM data (128-by-20 pixels) and the further processed ones (40-by-20 pixels, and with fixed position in each image). The performance was also compared with the existing neural networks (NNs)-based method. It was found that when DDM data are adequately preprocessed CNNs and NNs share similar accuracy, otherwise the former outperforms the latter. Further conclusion was thus drawn that CNNs were more tolerant to the data format changes than NNs.**

I. Introduction

Due to a decrease of sea ice cover in the North, shipping and offshore operations in these regions grow steadily [1]. A good knowledge of sea ice is thus critical for managing and protecting activities in such areas. With a higher and faster coverage, remote sensing techniques can be more efficient than *in-situ* measurements for obtaining sea ice information.

With millions of accessible TechDemoSat-1 (TDS-1) delay-Doppler maps (DDMs), great interest has been raised in sea ice remote sensing within Global Navigation Satellite System Reflectometry (GNSS-R) society, e.g., [2]–[4]. Recently, deep learning (DL) has been widely recognized as an excellent technique for remote sensing image processing [5] because it is able to learn features directly from data. Furthermore, convolutional neural networks (CNNs) have surpassed most DL algorithms in visual recognition [5]. It has been successfully applied to sea ice remote sensing using e.g. synthetic aperture radar [6] and altimeter [7] data. However, to the authors' best knowledge, the application of CNN in GNSS-R area has not yet been conducted. In this study, the technique of CNN is applied to TDS-1 DDMs for the first time, dedicated to detecting sea ice.

II. Structure of CNN for Sea Ice Detection

The preprocessing of DDM data follows the procedures in [4]. It should be noted that the positions of DDM specular points are not aligned in images (see Fig. 1) due to variation in path length. It is believed that CNN is able to extract the features independent of DDM's position. To demonstrate this, two different CNN structures are devised, which employ full (128-by-20 pixels) and cropped (40-by-20 pixels, the adopted signal box by [4]) DDM images as input, respectively. The framework of the employed CNN is presented in Fig. 2. It contains one convolution layer followed by one pooling layer and two fully connected layers. The convolution layer is with five 7×7 filters. Take the full-size input for illustration, the convolved images are of size (122, 14, 5) and the one resulting from the kth ($k = 1, ..., 5$) filter $\mathbf{W^k}$ can be described by

$$\begin{aligned} &\mathbf{h}_{ij}^{k} = \varphi((\mathbf{W}^{k} * \mathbf{X})_{ij} + b), \\ &i = 1, ..., 122, \ j = 1, ..., 14, \end{aligned} \tag{1}$$

where $\mathbf{X}$ and b are the input image and the bias. The convolution operation is denoted by $*$ and the activation function by φ. The widely adopted ReLU is chosen for φ i.e.

$$\varphi(z) = \max(0, z). \tag{2}$$

The max pooling layer is of pooling size (2, 2) and stride 2 [6]. This layer preserves the max value of every non-overlapped 2×2 block in the feature map to generate a sub-sampled one of size (61, 7, 5). The first fully connected layer is thus of dimension 2315 (= $61 \times 7 \times 5$). The second fully connected layer is equipped with 3 units. The structure of fully connected layers are quite similar with those of hidden layers in NNs, and for conciseness, find detailed formulations in [4]. The output layer is designed with 2 units a_1 and a_2, and the activation

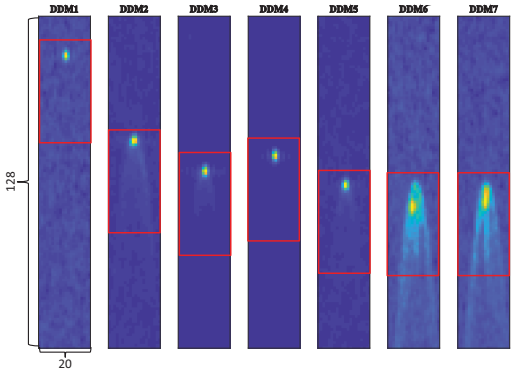

Fig. 1. DDM samples in its original data format (128×20), note that their specular points are not aligned. Red boxes indicate the cropped inputs (40×20) with settled position within each frame, following the fashion in [4]. Delay axes are in vertical and Doppler axes in horizontal.

978-1-5386-1338-2/18/$31.00

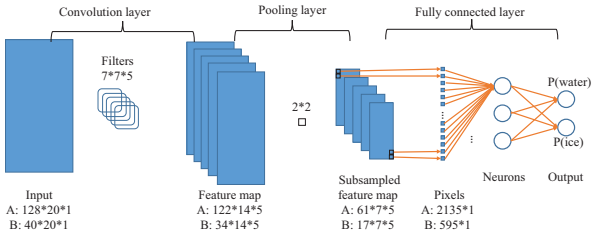

Fig. 2. Employed CNN structure in this work. Set A parameters are associated with full DDM input and set B for cropped input.

TABLE I
ACCURACY OF ICE DETECTION

ID	Number	Full-size input		Cropped input	
		CNN	NN	CNN	NN
RD 17 (training)	8377	99.15%	99.60%	99.03%	99.13%
RD 18 (test)	6071	98.12%	97.94%	98.94%	99.01%
RD 19 (test)	4915	97.97%	97.29%	98.77%	98.54%
RD 23 (test)	4799	96.42%	93.98%	98.41%	98.04%
RD 27 (test)	8522	97.04%	95.97%	98.43%	98.41%
	Average	97.83%	97.17%	98.73%	98.67%

function is the softmax function, which gives the probability of occurrence of sea ice or seawater,

$$p_r = \exp(a_r) / \sum_{s=1}^{2} \exp(a_s), \text{ where } r = 1, 2. \quad (3)$$

The detection result is based on the one with higher value.

It should also be noted that the overall layout of CNNs is the same when a cropped DDM is used as input, only the size of each layer needs to be adjusted accordingly and this can be readily deduced and has been given in Fig. 2 as set B.

III. RESULTS

To facilitate the comparison between accuracy of the proposed CNN-based and the existing NN-based sea ice remote sensing methods from DDM images, the same DDM datasets from [4] were employed. The reference SIC data were from passive microwave sensors [8] and were processed in the same manner as [4]. The target output was labelled as "sea ice" if the reference SIC was above 5%, otherwise, it was identified as "seawater". This threshold was selected based on the minimum detectable SIC from DDMs, which was found to be 5% [4].

Back-propagation learning and stochastic gradient descendant with momentum algorithm are adopted for training. A detailed derivation for this process can refer to [6]. After training, the sea ice detection-orientated CNNs were tested using the same data as those in [4], and the results are tabulated in Table I, in which the outcomes resulting from the full-size and cropped inputs are both presented.

From Table I, the proposed CNN-based sea ice detection method shows overall improved accuracy over the existing NN-based one, especially when using the original input size. An advantage of CNN lies in the usage of filters in the convolution layer and they appeared to reduce noise for DDM input in this work. The deployment of the convolution and pooling layers makes CNN less sensitive to disalignment of DDM specular point within a frame. Note that a pooling layer of size (2, 2) and stride 2 is able to resolve 1-pixel fluctuation. The resistance to the unsettlement relies on the depth and size of the convolution and pooling layers. As only one layer of each was adopted in this work, the ability of the designed CNN to be completely independent from the data locations is quite limited. This also accounts for the varied precision among different datasets since the degree of fluctuation differs. Still, CNN outperforms NN with original DDM format as discussed above and its performance may be further enhanced with more layers. When the data are adequately processed by cropping the DDM for alignment, both CNN and NN manifest good reliability. In addition to the advancement in accuracy, the designed CNNs are with fewer parameters than NNs, which makes the training easier [6]. The designed CNN is with 6666 parameters, while the NN is with 7691 for full-size input; and those for cropped images are 2046 and 2411, respectively.

IV. CONCLUSIONS

CNN is applied here for sea ice detection using TDS-1 DDMs. The devised scheme was found to be more advantageous than the current NN-based one in terms of 1) overall improved accuracy, 2) fewer parameters in the network (easier to train), and 3) more tolerant to changes in input data structure (requires less data preprocessing). In the future, more layers can be introduced and more training samples should be involved to further improve the accuracy.

ACKNOWLEDGMENT

This work was supported by the Natural Sciences and Engineering Research Council of Canada Discovery Grants (NSERC RGPIN-2017-04508 and RGPAS-2017-507962).

REFERENCES

[1] O. M. Johannessen, V. Y. Alexandrov, V. Alexandrov, I. Y. Frolov, and L. P. Bobylev, *Remote Sensing of Sea Ice in the Northern Sea Route*. Chichester, U.K.: Praxis Publishing Limited, 2007.

[2] Q. Yan and W. Huang, "Spaceborne GNSS-R sea ice detection using delay-Doppler maps: First results from the UK TechDemoSat-1 mission," *IEEE J. Sel. Topics Appl. Earth Observ. Remote Sens.*, vol. 9, no. 10, pp. 4795-4801, Oct. 2016.

[3] A. Alonso-Arroyo, V. U. Zavorotny, and A. Camps, "Sea ice detection using UK TDS-1 GNSS-R data," *IEEE Trans. Geosci. Remote Sens.*, vol. 55, no. 9, pp. 4989-5001, Sep. 2017.

[4] Q. Yan, W. Huang, and C. Moloney, "Neural networks based sea ice detection and concentration retrieval from GNSS-R delay-Doppler maps," *IEEE J. Sel. Topics Appl. Earth Observ. Remote Sens.*, vol. 10, no. 8, pp. 3789-3798, Aug. 2017.

[5] L. Zhang, L. Zhang, and B. Du, "Deep learning for remote sensing data: A technical tutorial on the state of the art," *IEEE Geosci. Remote Sens. Mag.*, vol. 4, no. 2, pp. 22-40, Jun. 2016.

[6] L. Wang, K. A. Scott, L. Xu, and D. A. Clausi, "Sea ice concentration estimation during melt from dual-pol SAR scenes using deep convolutional neural networks: A case study," *IEEE Trans. Geosci. Remote Sens.*, vol. 54, no. 8, pp. 4524-4533, Aug. 2016.

[7] X. Shen *et al.*, "Sea ice classification using Cryosat-2 altimeter data by optimal classifier-feature assembly," *IEEE Geosci. Remote Sens. Lett.*, vol. 14, no. 11, pp. 1948-1952, Nov. 2017.

[8] D. J. Cavalieri, C. Parkinson, P. Gloersen, and H. J. Zwally, "Sea ice concentrations from Nimbus-7 SMMR and DMSP SSM/I passive microwave data," Boulder, CO: Nat. Snow Ice Data Center, 1996.